

# Complete complementarity relations in tree level QED processes

Massimo Blasone, Silvio De Siena\*, Gaetano Lambiase, Cristina Matrella and Bruno Micciola<sup>1, 2, †</sup>

<sup>1</sup>*Dipartimento di Fisica, Università di Salerno, Via Giovanni Paolo II, 132 I-84084 Fisciano (SA), Italy*

<sup>2</sup>*INFN, Sezione di Napoli, Gruppo collegato di Salerno, Italy*

(Dated: September 24, 2024)

We exploit the complete complementarity relations (CCR) to fully characterize various aspects of quantumness in QED scattering processes at tree level. As a paradigmatic example, we consider Bhabha scattering in two different configurations: in the first case, the initial state is factorized in the spin and we study the generation of entanglement due to the scattering. Then we consider the most general case in which the initial state can be entangled: we find that the scattering generates and distributes quantum information in a non-trivial way among the spin degrees of freedom of the particles, with CCR relations being preserved. An important outcome of our analysis is that maximal entanglement is conserved in the scattering process involving only fermions as input and output states, with a more complex situation if photons are present.

PACS numbers:

## I. INTRODUCTION

In the last 25 years the development of quantum information theory has highlighted the pivotal role of the concept of entanglement, describing correlations of exclusive quantum nature, as the watershed with respect to classical phenomena where such kind of correlations cannot be generated at all. Entanglement is the object of very active research, due to its conceptual relevance in basic science and for being a resource for quantum technologies, such as quantum teleportation [1], quantum cryptography [2], quantum computation [3] and quantum metrology [4]. Parallel to the development of quantum information, entanglement has proved very useful in other scientific areas, as the study and characterization of quantum phase transitions [5] and, in quantum field theory (QFT), scaling laws [6] and conformal field theories [7]. The idea that entanglement can be exploited as a probe to investigate the deepest quantum nature and hidden mechanisms of fundamental interactions is gaining ground more and more. In mesonic (in particular, kaonic) systems, violations of Bell inequalities and presence of entanglement have been connected with discrete symmetries and special relativity probes [8]-[15], and in QCD entanglement suppression has been related with approximated spin-flavor symmetries [16]. Entanglement in top-antitop quark events produced at LHC has been recently observed [17, 18]. Quantum correlations, including entanglement, have also been extensively investigated in the context of neutrino oscillations [19]-[31]. Another line of investigation concerns the role of entanglement in particle processes as a probe for physics beyond standard model [32]-[34]. Finally, a vast literature has been devoted to investigate hidden contents of non-classicality in Gravity [35]-[44].

A great attention has been recently devoted to the study of entanglement in QFT scattering and decay processes as in Refs. [45]-[68]. In particular, a systematic investigation of the entanglement generation and distribution in fundamental processes has been recently developed in Refs. [66, 67] and [68]. In Refs. [66, 67], entanglement has been studied at tree level in QED and in electroweak processes, with the aim of showing that the constraint on the coupling structure of QED and weak interactions introduced by requiring maximal entanglement between helicity degrees of freedom, can lead to extract significant physical aspects of these fundamental theories. A systematic analysis of helicity entanglement generation in QED scattering processes has been carried out in Ref. [69]-[71] and, in particular, in Ref. [69] it has been studied for all energies and for arbitrary initial mixtures of helicity states. The analysis was performed at tree-level and one-loop contributions were estimated to be small.

In this paper we perform a complete study of entanglement in helicity for QED scattering processes at tree level. We do this by exploiting the so-called complete complementarity relations (CCR) which have already shown to be very useful in characterizing neutrino oscillations [30, 31]. The CCR incorporate into a conservation constraint all the complementary aspects which can be associated to a bipartite quantum system (in a pure or mixed state): predictability, local coherence (visibility) and nonlocal correlation (nonlocal coherence). The CCR establish that

\* Università degli Studi di Salerno (Ret. Prof.), email: silvio.desiena@gmail.com

†Electronic address: blasone@sa.infn.it; Electronic address: lambiase@sa.infn.it; Electronic address: cmatrella@unisa.it; Electronic address: bmicciola@unisa.it

the sum of the squares of these three quantities remains constant, and provide a tool to study the generation and transformation of such three quantities in consequence of a physical interaction. Equipped with this tool, we show that a QED scattering process modifies and distributes quantum information in a non-trivial way among the spin degrees of freedom of the particles, with the CCR fulfilled both for initial and final states.

We concentrate our analysis on the Bhabha scattering process as paradigmatic case, and we study other QED processes for the particularly interesting instance of initial maximally entangled states. For the simplest case of an initial factorized state, as e.g.  $|RL\rangle$  where  $R, L$  indicate helicity eigenstates, generation of entanglement has been already discussed in Ref.[66]: however, the use of CCR allows us to provide a complete characterization of the final state by revealing that entanglement generation is indeed related to the interplay between the three terms of CCR, depending on the scattering parameters.

We proceed in our analysis by considering more complex input states, which include an initial amount both of predictability and of local coherence in the two single-particle systems. Finally, we consider the most general initial state, in which the incoming particles can be entangled. In this case we can summarize the principal results as follows. If the initial state is maximally entangled, the QED processes involving only fermions as input and output states preserve maximal entanglement, while a more complex situation occurs if also photons are present. In the case of non-maximally entangled initial states we find behaviors in which, for a particular class of states, the entanglement is greater than the initial one, while for others it can be partially, or even totally, suppressed for any scattering angle (we define such regimes as *entanglophilus* and *entanglophobus*, respectively). For other configurations mixed behavior is detected. Finally, we have estimated entanglement as a *quantum resource* generated in the scattering process, by considering the average CCR terms per particle in a given domain of the scattering angle.

The paper is organized as follows. In section II we briefly review the complete complementarity relations. In section III we study Bhabha scattering with the CCR relations for the different classes of initial states. In section IV A we analyze the outputs of initial maximally entangled states for various QED processes. In section IV B we show the different classes in which can be partitioned the non-maximally entangled states. In section V A we study the entanglement as a resource in various regions of the scattering angle, and in section V B we provide some interpretation. Finally, in section VI, we discuss the results along with conclusions and outlook.

## II. COMPLETE COMPLEMENTARITY RELATIONS

In 1927 Niels Bohr conceived his complementarity principle [72], which states that a quantum system may possess properties which are equally real but mutually exclusive, in the sense that more information one has about one aspect of them, the less information can be obtained about the other. The concept of complementarity is often associated with wave-particle duality, the complementarity aspect between propagation and detection of a “quanton” [73].

The first quantitative version of Bohr’s principle, originally formulated in the context of the two-slit experiment, is due to Wootters and Zurek [74], who studied the effect of introducing a path-detecting device in a two-slit interference experiment, as originally proposed by Einstein. They showed that, by obtaining partial information about the quanton’s path, the interference pattern was only partially destroyed. The extension of this work by Englert [75] led to the duality relation:

$$D^2 + V^2 \leq 1, \quad (1)$$

where  $D$  represents the *path-distinguishability*, which measures the particle content, and  $V$  is the *visibility* of the interference. This led to the following relation:

$$P^2 + V^2 \leq 1, \quad (2)$$

where  $P$  is called *predictability*, representing a measure of the path information which still quantifies the particle aspect, and  $V$  is the visibility before defined.

Thus, the concept of complementarity associated with wave-particle duality is related to mutually exclusive properties of single-partite quantum systems. Eqs.(1) and (2) are only saturated for single-partite pure states, while for mixed states the strict inequality holds. In fact, Jacob and Bergou [76? , 77] have shown that for bipartite states a third entry, represented by a measure of correlation  $C$  between subsystems, has to be considered. This is because in general, even if the global state is pure, the states of subsystems can be mixed, implying a lack of information about the single subsystem: the missing information must be recovered in the correlations between subsystems. In this way it is possible to obtain a *complete complementarity relation* (CCR) for pure states, given by:

$$P_k^2 + V_k^2 + C^2 = 1, \quad (3)$$

where  $P_k$  and  $V_k$  are the predictability and the visibility referred to the single subsystem  $k$ , with  $k = 1, 2$  and  $C$  is a measure of non-local correlation. In Ref.[77]  $C$  represents the concurrence, a measure of entanglement.

Let us consider a general two-qubit pure quantum state:

$$|\psi\rangle = a|00\rangle + b|01\rangle + c|10\rangle + d|11\rangle, \quad (4)$$

with  $|a|^2 + |b|^2 + |c|^2 + |d|^2 = 1$ . The predictability  $P_k$  and visibility  $V_k$  are defined, respectively, as:

$$P_k = |\langle\psi|\sigma_{z,k}|\psi\rangle|, \quad \sigma_{z,k} = \begin{pmatrix} 1 & 0 \\ 0 & -1 \end{pmatrix}, \quad (5)$$

$$V_k = 2|\langle\psi|\sigma_k^+|\psi\rangle|, \quad \sigma_k^+ = \begin{pmatrix} 0 & 1 \\ 0 & 0 \end{pmatrix}, \quad (6)$$

Finally, the concurrence is defined as  $C = |\langle\psi|\tilde{\psi}\rangle|$ , where  $\tilde{\psi} = (\sigma_y \otimes \sigma_y)|\psi^*\rangle$ ,  $\sigma_y$  is the Pauli matrix and  $|\psi^*\rangle$  is the complex conjugate of  $|\psi\rangle$ . For the state in Eq.(4) these quantities are given by:

$$P_1 = (|c|^2 + |d|^2) - (|a|^2 + |b|^2), \quad P_2 = (|b|^2 + |d|^2) - (|a|^2 + |c|^2). \quad (7)$$

$$V_1 = 2|ac^* + bd^*|, \quad V_2 = 2|ab^* + cd^*|. \quad (8)$$

$$C(\psi) = 2|ad - bc|. \quad (9)$$

It is simple to verify from Eqs.(7)-(9) that the complete complementarity relation Eq.(3) is satisfied for a general pure bipartite state  $|\psi\rangle$ .

Thus, we deal with a *triality relation* formed by two quantities generating *local* single-partite realities which can be related to wave-particle duality, and a correlation measure which generates an exclusive bipartite *non-local* reality. CCR as in Eq.(3) are valid only if the whole system is in a pure state. When a mixed state is considered the CCR becomes:

$$P_k^2 + V_k^2 + C^2 \leq 1. \quad (10)$$

This can be explained by considering that the correlation measure and the visibility for pure states represent upper bounds for the corresponding quantities for mixed states.

Recently, in Refs. [78–80] CCR have been reformulated and extended in a form which is particularly suitable for our purposes. We then briefly review, for the case of a bipartite pure state, the main aspects of this approach which efficiently expresses CCR in terms of the density matrix of the system.

Let us consider a bipartite pure state in the Hilbert space  $\mathcal{H}_{AB} = \mathcal{H}_A \otimes \mathcal{H}_B$  of dimension  $d = d_A d_B$ , where  $d_A$  and  $d_B$  are the dimensions of  $\mathcal{H}_A$  and  $\mathcal{H}_B$ , respectively. The density matrix associated to this state can be written as:

$$\rho_{AB} = \sum_{i,k=0}^{d_A-1} \sum_{j,l=0}^{d_B-1} \rho_{ij,kl} |i, j\rangle_{AB} \langle k, l|. \quad (11)$$

By tracing over B we obtain the reduced density matrix for subsystem A:

$$\rho_A = \sum_{i,k=0}^{d_A-1} \rho_{ik} |i\rangle_A \langle k|. \quad (12)$$

It is important to point out that, on the basis of measures we choose for predictability and visibility and consequently for the correlation term, we can define different forms of CCR. As an example, here we show two possible forms:

$$P_{hs}(\rho_A) + C_{hs}(\rho_A) + C_{hs}^{nl}(\rho_{A|B}) = \frac{d_A - 1}{d_A}, \quad (13)$$

$$P_{vn}(\rho_A) + C_{re}(\rho_A) + S_{vn}(\rho_A) = \log_2 d_A. \quad (14)$$

In Eq.(13) predictability, visibility and nonlocal coherence are expressed in terms of the Hilbert-Schmidt measures, given by

$$P_{hs}(\rho_A) = \sum_{i=0}^{d_A-1} (\rho_{ii})^2 - \frac{1}{d_A}, \quad (15)$$

$$C_{hs}(\rho_A) = \sum_{i \neq k}^{d_A-1} |\rho_{ik}|^2, \quad (16)$$

$$C_{hs}^{nl}(\rho_{A|B}) = \sum_{i \neq k, j \neq l} |\rho_{ij,kl}|^2 - 2 \sum_{i \neq k, j < l} \text{Re}(\rho_{ij,kj} \rho_{il,kl}^*). \quad (17)$$

In Eq.(14), the predictability is expressed in terms of the von Neumann entropy as  $P_{vn}(\rho_A) = \log_2 d_A - S_{vn}(\rho_{A,diag})$  and  $C_{re}(\rho_A) = S_{vn}(\rho_{A,diag}) - S_{vn}(\rho_A)$  is the relative entropy of coherence.  $S_{vn}(\rho_A)$  is the von Neumann entropy of entanglement.

Referring to the entropic form of CCR given in Eq.(14), for completeness we briefly show also the CCR relation for the case of a global mixed state. In this case  $S_{vn}(\rho_A)$  cannot be considered as a measure of entanglement between A and B, but it just represents a measure of uncertainty of A. Then, the correlation between A and B is quantified by the sum of two terms, given respectively by the mutual information  $I_{A:B}(\rho_{AB})$ , a measure of the total correlation between A and B, and by the conditional entropy  $S_{A|B}(\rho_{AB})$ , which quantifies the ignorance about the whole system one has by looking only at subsystem A. Thus, for a global bipartite mixed state, the entropic form of CCR becomes:

$$P_{vn}(\rho_A) + C_{re}(\rho_A) + S_{A|B}(\rho_{AB}) + I_{A:B}(\rho_{AB}) = \log_2 d_A. \quad (18)$$

Finally, for the general bipartite state Eq.(4), we add some more information on the form of the concurrence, on its relation with entropy measures (linear  $S_{lin}$  and von Neumann  $S_{vn}$  entropies), and on the maximum entanglement condition. If we write the coefficients in Eq.(4) in the following way:

$$a \equiv |a|, \quad b = |b| e^{i\xi}, \quad c = |c| e^{i\eta}, \quad d = |d| e^{i\tau}, \quad (19)$$

we obtain, for the squared concurrence and the quantum entropies the following expressions:

$$C^2 = 4 \{ |a|^2 |d|^2 + |b|^2 |c|^2 - 2 |a| |b| |c| |d| \cos [\xi - (\eta + \tau)] \}. \quad (20)$$

$$S_{lin} = 2(1 - \text{Tr}(\rho^2)) = C^2, \quad (21)$$

$$S_{vn} = -\rho \log_2 \rho = -\frac{1}{2} (1 + \sqrt{1 - C^2}) \log_2 \left[ \frac{1}{2} (1 + \sqrt{1 - C^2}) \right] - \frac{1}{2} (1 - \sqrt{1 - C^2}) \log_2 \left[ \frac{1}{2} (1 - \sqrt{1 - C^2}) \right]. \quad (22)$$

We see that the more general condition for maximum concurrence is

$$|a|^2 = |d|^2, \quad |b|^2 = |c|^2, \quad \xi - (\eta + \tau) = (2n + 1)\pi, \quad n \in \mathbb{Z}, \quad (23)$$

and that the maximum concurrence corresponds both to maximum linear entropy and to the maximum von Neumann entropy.

### III. CCR IN BHABHA SCATTERING PROCESS

We start by studying in detail the three quantities above introduced (predictability, local coherence and entanglement) for the specific case of Bhabha scattering at tree level for which entanglement generation was studied in Ref.[66].

In this Section we briefly recall the formalism used in Ref.[52] and Ref.[68]. From now on, we perform our calculations in the COM reference frame for particles A and B.

The internal product of fermion states is defined as

$$\langle k, a | p, b \rangle = 2E_{\mathbf{k}} (2\pi)^3 \delta^{(3)}(\mathbf{k} - \mathbf{p}) \delta_{a,b}, \quad (24)$$

where  $k$  and  $p$  are the 4-momenta and  $a$  and  $b$  are the spin indices.

For a generic initial state the final states can be expressed in terms of the scattering amplitudes  $\mathcal{M}(p_1, a, p_2, b; p_3, r, p_4, s)$ . For example, considering the simple initial state:

$$|i\rangle = |p_1, a\rangle_A \otimes |p_2, b\rangle_B, \quad (25)$$

the general final state results

$$|f\rangle = |i\rangle + i \sum_{r,s} \int \frac{d^3\mathbf{p}_3 d^3\mathbf{p}_4}{(2\pi)^6 2E_{\mathbf{p}_3} 2E_{\mathbf{p}_4}} \delta^{(4)}(p_1 + p_2 - p_3 - p_4) \left[ \mathcal{M}(a, b; r, s) |p_3, r\rangle_A \otimes |p_4, s\rangle_B \right],$$

where  $\mathcal{M}(a, b; r, s)$  represents the scattering amplitudes in which for simplicity we omit the initial and final momenta.

The partial trace operation is given by

$$Tr_X[\rho] = \sum_{\sigma} \int \frac{d^3\mathbf{k}}{(2\pi)^3 2E_{\mathbf{k}}} (\mathbb{I}_r \otimes {}_X\langle k, \sigma |) \rho (\mathbb{I}_r \otimes |k, \sigma\rangle_X), \quad (26)$$

where  $\mathbb{I}_r$  denotes the identity operation in the remaining subspaces,  $k$  and  $\sigma$  are the 4-momentum and spin indices as before and  $X$  is the generic space with respect to which we calculate the trace. So, we can describe the final states in terms of the density matrix:

$$\rho_{AB}^f = \frac{1}{\mathcal{N}} |f\rangle \langle f|, \quad (27)$$

where  $\mathcal{N}$  is the normalization constant. Using Eq.(26) and applying the following relations

$$2\pi\delta^{(0)}(E_i - E_f) = \int_{-T/2}^{T/2} e^{i(E_i - E_f)t} dt, \quad (28)$$

$$(2\pi)^3 \delta^{(3)}(\mathbf{k} - \mathbf{p}) = V \delta_{\mathbf{k}, \mathbf{p}}, \quad (29)$$

which imply that  $(2\pi)\delta^{(0)}(0) = T$  and  $(2\pi)^3 \delta^{(3)}(0) = V$ , we can easily compute the normalization constant  $\mathcal{N}$ :

$$\mathcal{N} = Tr_A \left[ Tr_B \left[ |f\rangle \langle f| \right] \right]. \quad (30)$$

In this work we study the change of the CCR's terms, relative to the spin degrees of freedom, between states before and after the scattering process at fixed momenta. as in Refs.[66]-[69], where it is assumed that an arbitrarily sharp filtering of the outgoing particles in momentum space is performed, without resolving their internal (helicity or polarisation) degrees of freedom. As remarked in Ref.[69], although being an idealisation, the filtering corresponds to a selection of the output momenta, and the entanglement between the helicity degrees of freedom at that given momenta is still a fundamental property of the output state of the quantum field upon scattering. So, from now on, we will consider these states in terms of helicity states.

### A. Factorized and polarized incoming states

We start with the simplest instance of an initial factorized state of two polarized particles:

$$|i\rangle_I = |R\rangle_A |L\rangle_B. \quad (31)$$

After the scattering, if we limit our attention to a selection of results at each fixed angle  $\theta \neq 0, 2\pi$ , up to a normalization factor, we can express the *final reference state* as <sup>1</sup>

$$|f\rangle_I = \sum_{r,s} \mathcal{M}(RL; rs) |r\rangle_A |s\rangle_B, \quad (32)$$

---

<sup>1</sup> The normalization can be fixed after the operation of momentum filtering (i.e. selection of the measurements relative to a specific scattering angle  $\theta$ ) that is formally described by applying a POVM operator as discussed in Ref.[69].

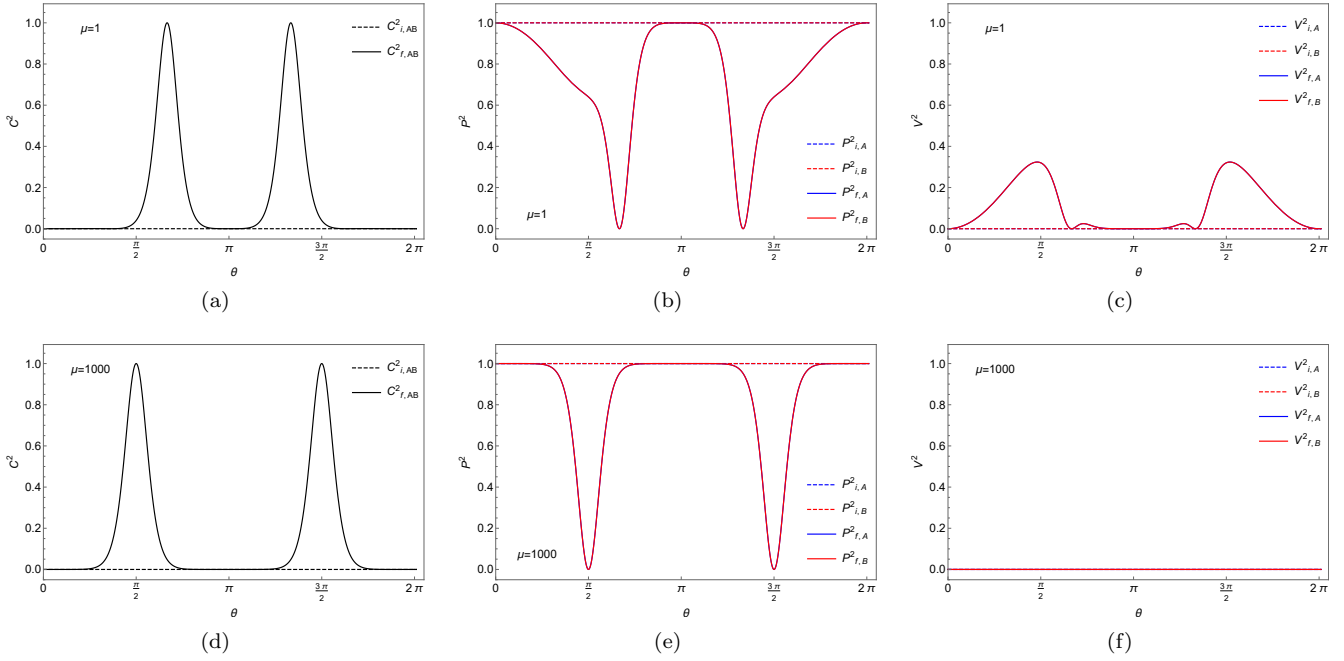


FIG. 1: Plot of the CCR terms  $C^2$ ,  $P^2$  and  $V^2$ , for initial and final states of Case I. Panels (a),(b),(c) refer to the value  $\mu = 1$  (non-relativistic regime). Panels (d),(e),(f) refer to the value  $\mu = 1000$  (relativistic regime).

where  $\mathcal{M}(RL; rs)$  are scattering amplitudes whose explicit form is reported in the Appendix.

The initial state  $|i\rangle_I$  is characterized by maximal predictability for both particles:  $P_{i,A} = P_{i,B} = 1$  and  $V_{i,A} = V_{i,B} = C_i = 0$ . We observe that, as a consequence of the scattering, other CCR terms develop at expense of the predictability, according to Eq.(3). This values change due to the scattering process, and in Fig.1 we report both the non-relativistic case (Figs.1a-1c) and the relativistic one (Figs.1d-1f) characterized by different values of  $\mu \equiv |\mathbf{p}|/m_e$ , where  $|\mathbf{p}|$  is the incoming momentum and  $m_e$  the electron mass.

As first important remark, we see that CCR as in Eq. (3) are verified after the scattering in any regimes. Equivalent results are obtained if one considers the entropic approach (Eqs.(13)-(14)). In particular, the general form expressed by Eq.(11), is obtained if one identify the density matrix elements as

$$\rho_{ij,kl} = \mathcal{M}(RL, ij)\mathcal{M}(RL, kl), \quad (33)$$

where  $i, j, k, l = R, L$  and  $\mathcal{M} \in \mathbf{R}$ .

Also we note that there is a symmetry between the two subsystems  $A$  and  $B$  for which predictability and visibility coincide. Moreover, comparing Fig.1c and Fig.1f we see that in the non-relativistic regime visibility develops, while it remains zero in the relativistic case.

## B. General factorized states

In this Section we consider a generalization of the previous case, in which the incoming particles are in a superposition of helicity states. We have that the initial state is again a product state, but with predictability and visibility different from zero:

$$|i\rangle_{II} = (\cos \alpha |R\rangle_A + e^{i\xi} \sin \alpha |L\rangle_A) \otimes (\cos \beta |R\rangle_B + e^{i\eta} \sin \beta |L\rangle_B). \quad (34)$$

A particular case of such an initial state, obtained for  $\alpha = 0$  and  $\xi = \eta = 0$ , has been studied in detail in Ref.[68].

The final state results

$$\begin{aligned} |f\rangle_{II} = \sum_{r,s} & \left[ \cos \alpha \cos \beta \mathcal{M}(RR; rs) |r\rangle_A |s\rangle_B + e^{i\eta} \cos \alpha \sin \beta \mathcal{M}(RL; rs) |r\rangle_A |s\rangle_B + e^{i\xi} \sin \alpha \cos \beta \mathcal{M}(LR; rs) |r\rangle_A |s\rangle_B \right. \\ & \left. + e^{i(\xi+\eta)} \sin \alpha \sin \beta \mathcal{M}(LL; rs) |r\rangle_A |s\rangle_B \right]. \end{aligned} \quad (35)$$

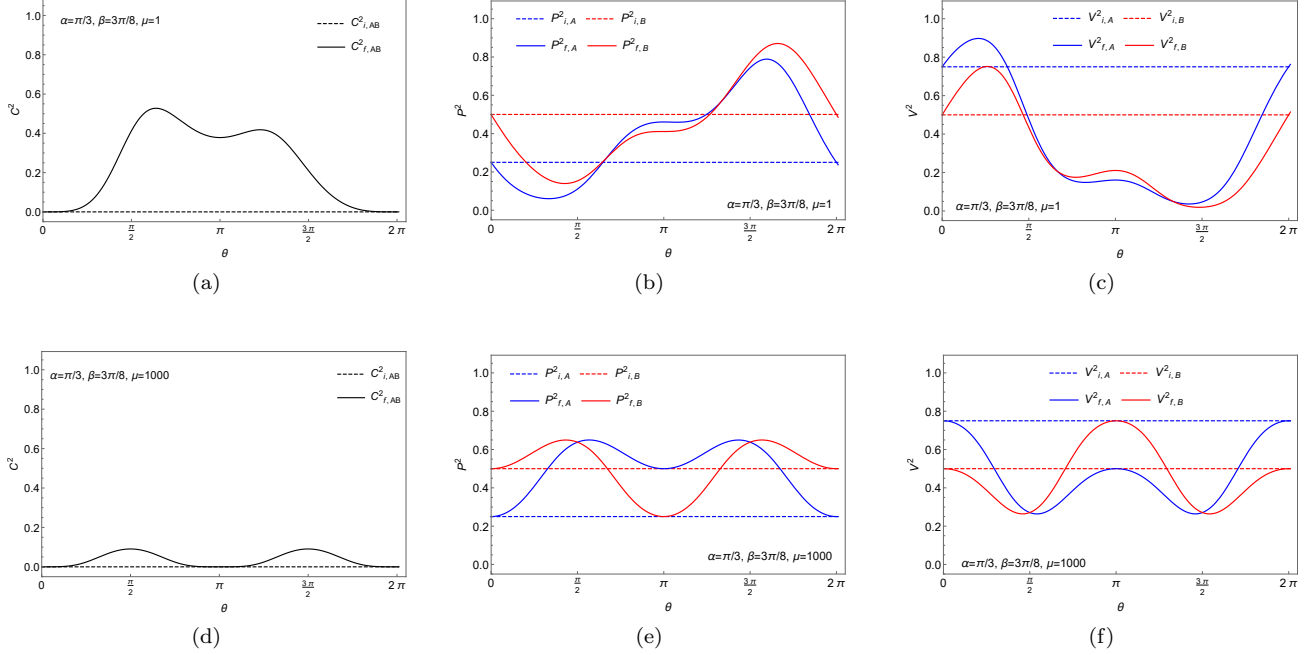


FIG. 2: Plot of the CCR terms  $C^2$ ,  $P^2$  and  $V^2$ , for initial and final states of Case II. Panels (a),(b),(c) refer to the value  $\mu = 1$  (non-relativistic regime). Panels (d),(e),(f) refer to the value  $\mu = 1000$  (relativistic regime).

For simplicity, we set  $\eta = \xi = 0$  and refer to Figs.2a-2c for the non-relativistic case, and to Figs.2d-2f for the relativistic one. It is simple to verify that Eq.(3) holds again. At variance with case I, in the non-relativistic regime we note that the symmetry between  $A$  and  $B$  is lost due to the asymmetry already present in the initial state, and the two parts show different predictability and visibility. Furthermore in this case, an asymmetry emerges with respect to the scattering angle  $\theta = \pi$ . It can be verified that this is a subtle consequence of the off-diagonal terms contributions.

In the relativistic case, symmetry with respect to  $\theta = \pi$  is restored, and visibility is non-zero simply because it is already non vanishing before the scattering. As in the previous case, we can verify Eq.(13), by promoting the matrix elements to the form

$$\rho_{i,j,k,l} = A_{\zeta,\kappa} A_{\zeta',\kappa'}^* \mathcal{M}(i,j,\zeta,\kappa) \mathcal{M}(k,l,\zeta',\kappa'), \quad (36)$$

where the repeated indices  $\zeta, \kappa = R, L$  are summed according to the Einstein convention and  $A_{R,R} = \cos \alpha \cos \beta$ ,  $A_{R,L} = e^{i\eta} \cos \alpha \sin \beta$ ,  $A_{L,R} = e^{i\xi} \sin \alpha \cos \beta$  and  $A_{L,L} = e^{i(\eta+\xi)} \sin \alpha \sin \beta$ . The form (36) is the most general one, and remains the same also in the next case C.

It is interesting to consider the relativistic limit  $\mu = \infty$  for which it is possible to obtain analytical forms of the CCR quantities for the state in Eq.(35):

$$\lim_{\mu \rightarrow \infty} C = \frac{4}{D_{II}} \left( 1 - 8 \cos [2(\alpha - \beta)] + 7 \cos [2(\alpha + \beta)] - 2 \cos 2\theta \sin^2 [\alpha + \beta] \right) \sin^2 \theta, \quad (37)$$

$$\lim_{\mu \rightarrow \infty} P_A = \frac{8}{D_{II}} \left[ \cos 2\beta (\cos 3\theta + 7 \cos \theta - 8) - \cos 2\alpha (\cos 3\theta + 7 \cos \theta + 8) \right], \quad (38)$$

$$\lim_{\mu \rightarrow \infty} P_B = \frac{8}{D_{II}} \left[ \cos 2\alpha (\cos 3\theta + 7 \cos \theta - 8) - \cos 2\beta (\cos 3\theta + 7 \cos \theta + 8) \right], \quad (39)$$

$$\lim_{\mu \rightarrow \infty} V_A = \frac{64}{D_{II}} \left( \cot^4 \frac{\theta}{2} \sin 2\alpha + \sin 2\beta \right) \sin^4 \frac{\theta}{2}, \quad (40)$$

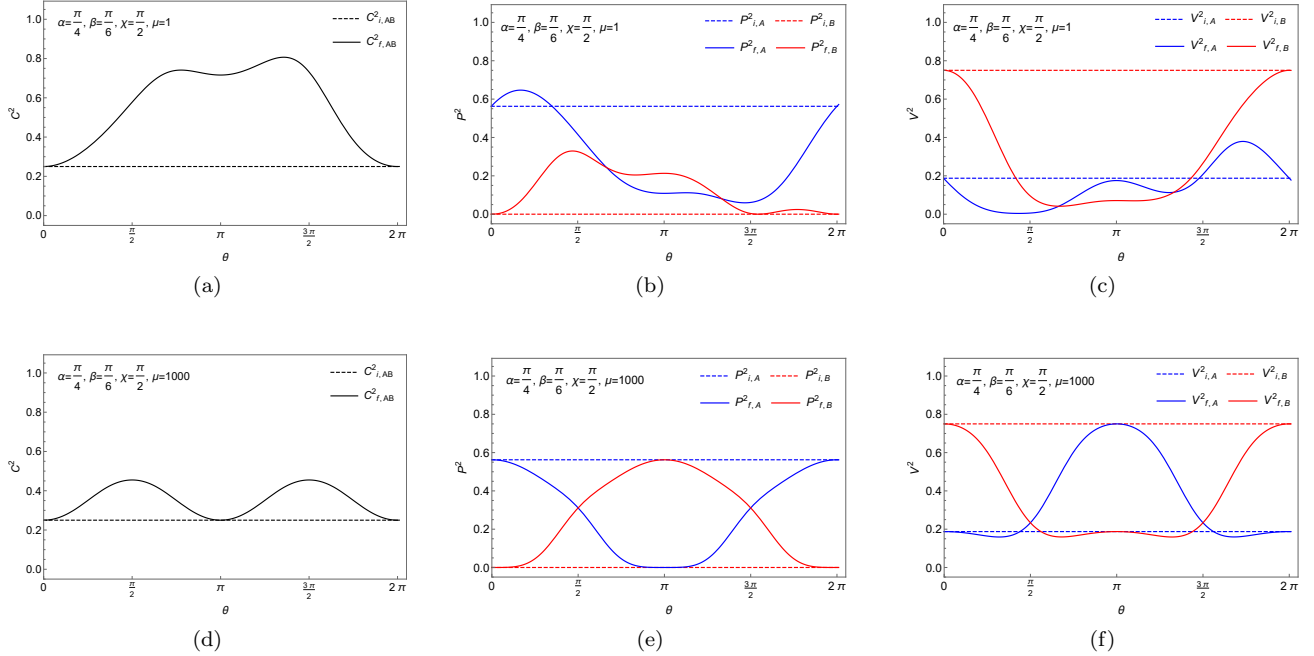


FIG. 3: Plot of CCR terms for Case III with low value of initial entanglement.

$$\lim_{\mu \rightarrow \infty} V_B = \frac{64}{D_{II}} \left( \cot^4 \frac{\theta}{2} \sin 2\beta + \sin 2\alpha \right) \sin^4 \frac{\theta}{2}. \quad (41)$$

with

$$D_{II} \equiv 2(7 + \cos^2 2\theta)^2 + 4 \cos 2\alpha \cos 2\beta (15 + \cos 2\theta) \sin^2 \theta + 8 \sin 2\alpha \sin 2\beta \sin^4 \theta \quad (42)$$

As it can be easily checked, the sum of the squares of this three quantities is exactly one, for each subsystem, according to Eq.(3).

### C. General incoming state

Finally we consider the case of the most general initial state, parameterized by six real parameters (three angles and three phases), and configurations in which entanglement is present from the beginning:

$$|i\rangle_{III} = \cos \alpha |R\rangle_A |R\rangle_B + e^{i\xi} \sin \alpha \cos \beta |R\rangle_A |L\rangle_B + e^{i\eta} \sin \alpha \sin \beta \cos \chi |L\rangle_A |R\rangle_B + e^{i\tau} \sin \alpha \sin \beta \sin \chi |L\rangle_A |L\rangle_B. \quad (43)$$

The corresponding final state is given by

$$|f\rangle_{III} = \sum_{r,s} \left[ \cos \alpha \mathcal{M}(RR; rs) |r\rangle_A |s\rangle_B + e^{i\xi} \sin \alpha \cos \beta \mathcal{M}(RL; rs) |r\rangle_A |s\rangle_B + e^{i\eta} \sin \alpha \sin \beta \cos \chi \mathcal{M}(LR; rs) |r\rangle_A |s\rangle_B + e^{i\tau} \sin \alpha \sin \beta \sin \chi \mathcal{M}(LL; rs) |r\rangle_A |s\rangle_B \right]. \quad (44)$$

The matrix elements  $\rho_{i,j,k,l}$  have the same form of Eq.(36) with  $A_{R,R} = \cos \alpha$ ,  $A_{R,L} = e^{i\xi} \sin \alpha \cos \beta$ ,  $A_{L,R} = e^{i\eta} \sin \alpha \sin \beta \cos \chi$  and  $A_{L,L} = e^{i\tau} \sin \alpha \sin \beta \sin \chi$ .

In the following we show that, for some choice of parameters, the entanglement resulting after the scattering process is in a non-trivial relation with respect to its initial value. We illustrate this by providing some significant examples. Consider the two configurations  $\mathcal{A} = (\alpha = \pi/4, \beta = \pi/6, \chi = \pi/2)$  and  $\mathcal{B} = (\alpha = \pi/3, \beta = \pi/6, \chi = 0)$ .

For the configuration  $\mathcal{A}$ , in Figs.3a-3c we plot the non-relativistic case, while Figs.3d-3f refer to the relativistic one. From Figs.3a and 3d we can see that entanglement increases in both non-relativistic and relativistic regimes.

On the other hand, when configuration  $\mathcal{B}$  is adopted (see Fig.4), we observe the opposite behaviour. In particular, in the non-relativistic regime, the final entanglement is strongly suppressed and for some values of  $\theta$  it vanishes.

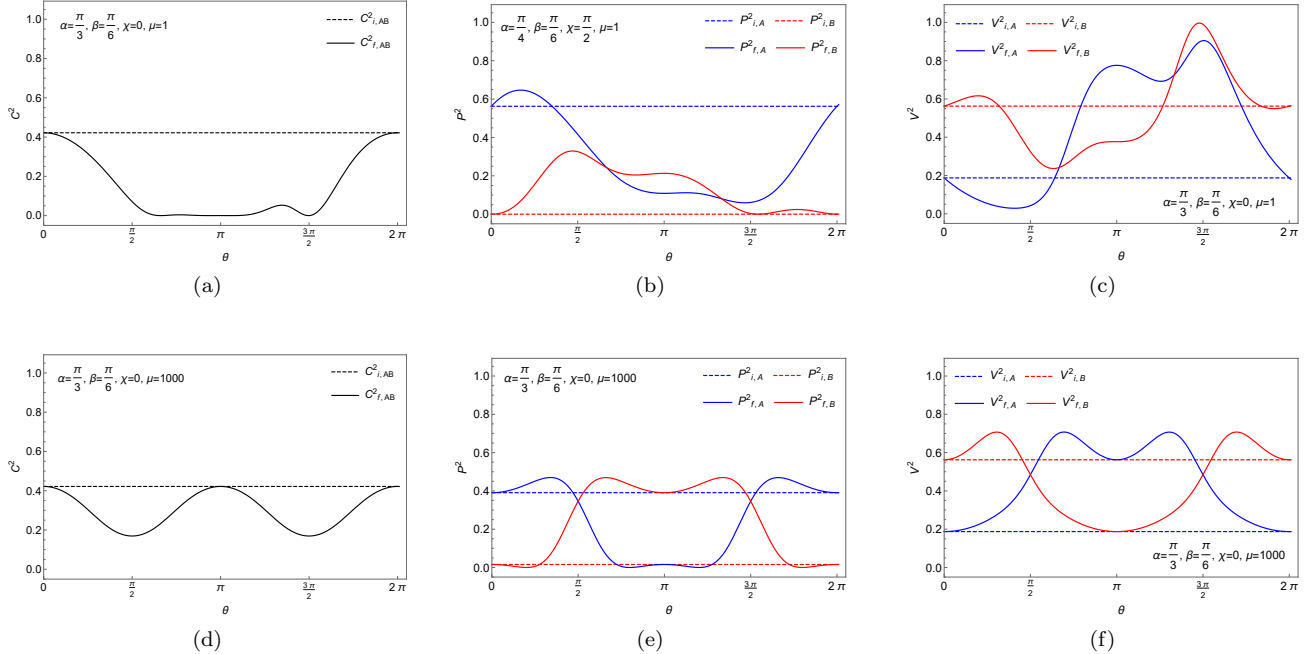


FIG. 4: Plot of CCR terms for Case III with nonzero initial value for all three quantities.

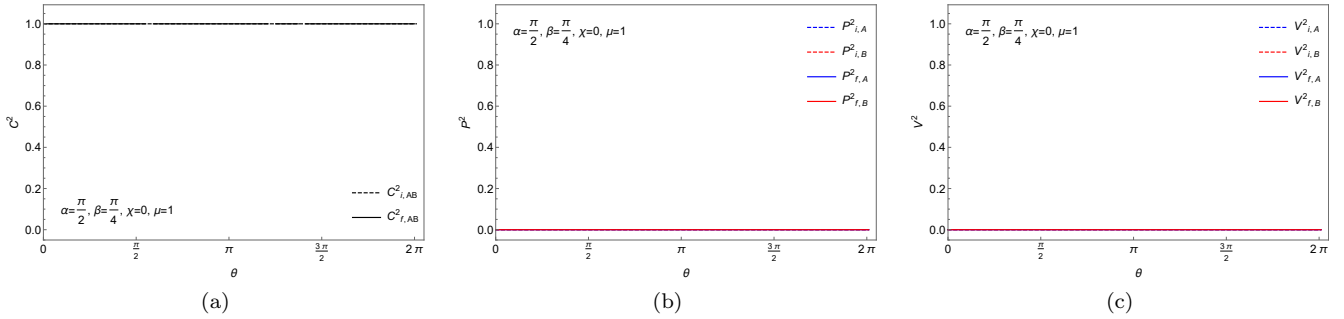


FIG. 5: Plot of CCR terms for Case III with initial Bell state.

#### IV. CLASSIFICATION OF INITIAL STATES BY ENTANGLEMENT BEHAVIOUR UNDER SCATTERING

The non-trivial behaviour of entanglement in the scattering processes, observed in the previous section, suggests to search for a classification of states with similar properties in this respect. In the following we show that one can identify three classes of states which we define as *entanglophilus*, *entanglophobous* and *mixed*. Furthermore, a very interesting situation arises when the initial state is maximally entangled.

##### A. Maximally entangled states

Following the discussion of Section III C, we consider as initial state the Bell state  $\Psi^+ = (|RL\rangle + |LR\rangle)/\sqrt{2}$ : from Fig.5, we see that the initial maximal entanglement is conserved at any  $\theta$  after the scattering process and, consistently, no visibility and predictability arise. This very remarkable behaviour induces us to investigate the case of generic maximally entangled initial states for Bhabha scattering and also for other QED processes. We consider separately four processes, in which only spin-1/2 massive particles are involved, and other two in which also spin-1 massless particles, as in- and out-states, are present (see tables below). By means of the scattering amplitudes reported in

Appendix we have verified that for the first four processes there is a complete conservation of maximum entanglement: if the input state is any maximally entangled state, then the final state is maximally entangled too, whatever the scattering angle and the value of  $\mu$  (*complete maximal entanglement conservation*). At variance, for the last two processes this is in general not true: for the process of annihilation  $e^-e^+ \rightarrow \gamma\gamma$  maximal concurrence conservation partially survives, while for the Compton process there is no conservation of maximal entanglement.

For any process it is clarifying to consider, as initial maximally entangled states, the four Bell states

$$\Phi^\pm = \frac{1}{\sqrt{2}}(|RR\rangle \pm |LL\rangle), \quad \Psi^\pm = \frac{1}{\sqrt{2}}(|RL\rangle \pm |LR\rangle). \quad (45)$$

with the corresponding final states. In the tables below we report the correspondences for each process:

Bhabha			Møller		
In. State	Fin. State	Conc.	In. State	Fin. State	Conc.
$\Phi^+$	$\Phi^+$	1	$\Phi^+$	$\cos s_3 \Phi^+ + \sin s_3 \Psi^-$	1
$\Phi^-$	$\cos s_1 \Phi^- + \sin s_1 \Psi^+$	1	$\Phi^-$	$\Phi^-$	1
$\Psi^+$	$\cos s_2 \Phi^- + \sin s_2 \Psi^+$	1	$\Psi^+$	$\Psi^+$	1
$\Psi^-$	$\Psi^-$	1	$\Psi^-$	$\cos s_4 \Phi^+ + \sin s_4 \Psi^-$	1

TABLE I: Bell states transformation and entanglement of final states for Bhabha and Møller scattering processes.

In the last table, referring to the Compton scattering, “GC” (Generic Coefficients) indicates that the coefficients of the four terms  $|rs\rangle$ , in which  $r,s = R,L$ , are all different, preventing a combination of Bell states with maximal concurrence. The angles  $\{s^i\}$  are suitably expressed in terms of the scattering amplitudes, for example, in the case of initial state  $\Phi^-$  in the Bhabha scattering,  $s_1 = \arccos[\mathcal{N}^{-1}(\mathcal{M}(RR;RR) - \mathcal{M}(RR;LL))]$ , where  $\mathcal{N} = \sqrt{(\mathcal{M}(RR;RR) - \mathcal{M}(RR;LL))^2 + 4\mathcal{M}(RR;LL)^2}$  is the normalization factor. Similarly for the other cases.

We see that the tables provide a sort of characterization of each process. The first four scattering processes convert the initial Bell states in themselves, or in a convex combination of Bell states again with concurrence one, which keep the same superposition form if the process is repeated <sup>2,3</sup>.

We consider now the last two processes involving photons. For the process of annihilation in two photons we see that maximum concurrence is conserved for all the values of the parameters only for three Bell states as initial states, while  $\Phi^-$  goes in a combination with maximal concurrence achieved only for some values of the parameters. For the Compton process we see that conservation of maximal entanglement is not allowed at all. It is important to underline that in the case of the Compton scattering the interaction never generates a maximally entangled state as also found in Ref.[67].

### B. Entanglophilus, Entanglophobus and mixed regimes

Coming back to the two configurations  $\mathcal{A}$  and  $\mathcal{B}$  introduced in sec.III C, we can identify the entanglophilus, entanglophobus and mixed regimes in a more systematic way. In order to characterize such patterns let us again restrict to the Bhabha scattering and, starting from the two pairs of Bell states in Eq.(45), we consider the states parameterized by the angles  $\alpha$  and  $\beta$  (see Eq.(43)) and defined by:

$$\Phi_\alpha^\pm \equiv \cos \alpha |RR\rangle \pm \sin \alpha |LL\rangle; \quad \Psi_\beta^\pm \equiv \cos \beta |RL\rangle \pm \sin \beta |LR\rangle. \quad (46)$$

<sup>2</sup> The achievement of a final, no more changed, combination with maximum concurrence is the common mechanism. For example, if as initial states one chooses the generalized Bell states with a relative phase different from  $0, \pi$ , the final combination of concurrence 1 is achieved after two iterations.

<sup>3</sup> For the process of annihilation in muons we recall that it can be realized only in ultrarelativistic regime, and thus only Bell states  $\Psi^\pm$  can be taken into account. However, for completeness we have added also as hypothetical initial states the Bell states  $\Phi^\pm$ . We see that, just hypothetically, they would preserve concurrence 1, although the process would be “transparent” for the state  $\Phi^+$  in the sense that the first tree-level correction would result to be zero.

	$e^-e^+ \rightarrow \mu^-\mu^+$			$e^-\mu^- \rightarrow e^-\mu^-$	
In. State	Fin. State	Conc.	In. State	Fin. State	Conc.
$\Phi^+$	$\Phi^+$	1	$\Phi^+$	$\cos s_7 \Phi^+ + \sin s_7 \Psi^-$	1
$\Phi^-$	$\cos s_5 \Phi^+ + \sin s_5 \Psi^-$	1	$\Phi^-$	$\cos s_8 \Phi^- + \sin s_8 \Psi^+$	1
$\Psi^+$	$\cos s_6 \Phi^+ + \sin s_6 \Psi^-$	1	$\Psi^+$	$\cos s_9 \Phi^- + \sin s_9 \Psi^+$	1
$\Psi^-$	$\Psi^-$	1	$\Psi^-$	$\cos s_{10} \Phi^+ + \sin s_{10} \Psi^-$	1

TABLE II: Bell states transformation and entanglement of final states for electron-positron annihilation in two muons (see footnote [83]) and electron-muon in electron-muon scattering processes.

	$e^-e^+ \rightarrow \gamma\gamma$			Compton	
In. State	Fin. State	Conc.	In. State	Fin. State	Conc.
$\Phi^+$	$\Phi^-$	1	$\Phi^+$	GC	< 1
$\Phi^-$	$\cos r \Phi^+ + \sin r \Psi^+$	$ \sin(2r) $	$\Phi^-$	GC	< 1
$\Psi^+$	$\Psi^+$	1	$\Psi^+$	GC	< 1
$\Psi^-$	$\Psi^-$	1	$\Psi^-$	GC	< 1

TABLE III: Bell states transformation and entanglement of final states for electron-positron annihilation in two photons and Compton scattering processes.

If, for low initial momenta, one lowers the  $\alpha$ -parameter from  $\pi/4$  up to zero in  $\Phi_\alpha^+$ , it results that after the scattering the entanglement will be greater than its initial value for every  $\theta$ : this identifies the regime that we termed as *entangophilus*. Such behavior qualitatively persists also in the relativistic regime, although much attenuated. By performing a similar analysis for the state  $\Phi_\alpha^-$ , we find lower entanglement in the final state previous defined as *entangophobus* regime.

The situation is summarized in Fig.6, where we plot the relative difference between final and initial entanglement of states  $\Phi_\alpha^+$  and  $\Phi_\alpha^-$  defined as  $\Delta C \equiv (C_f - C_i)/C_i$ .

A similar analysis can be extended to the states  $\Psi_\beta^\pm$ . In this case we find an intermediate situation, the *mixed* regime, between the last two. It is interesting to note that these cases, described in Fig.7, are not symmetric under the change of sign in the  $\beta$ -parameter.

## V. DISCUSSION

In light of these results, two questions naturally arise: Can we consider and quantify the interaction due to the scattering process as a valuable resource for generating and transferring entanglement? Secondly, how can these results be interpreted? In the following two subsections, we address these questions.

### A. Entanglement resource

In order to understand if the scattering process can be considered a good resource to create pairs of entangled particles we report, as a paradigmatic example, the analysis of the entanglement generation starting from the simplest cases *I* and *II* at various energy regimes. To this aim, we have to know how many particles will be scattered in that domains of scattering angle  $\theta$  for which the entanglement is significantly different from zero. We can identify such domains from the plot previously reported. For what concerns the number of particles in output, we know that it is proportional to the differential cross section. As shown in Ref.[81], for a  $2 \rightarrow 2$  scattering process where all four masses involved are identical, in the COM reference frame the differential cross section results:

$$\frac{d\sigma}{d\Omega} = \frac{|\mathcal{M}|^2}{64\pi^2 E_{CM}^2}. \quad (47)$$

So, in order to estimate and characterize the entanglement as a real resource, we have chosen to weight the three CCR terms with the number of particles in the  $\theta$ -domain of interest defining the weighted averages as:

$$\overline{Q^2} = \frac{1}{N} \sum_{rs} \int_{\mathcal{D}} |M(a, b; r, s)|^2 Q^2(\theta) d\theta, \quad (48)$$

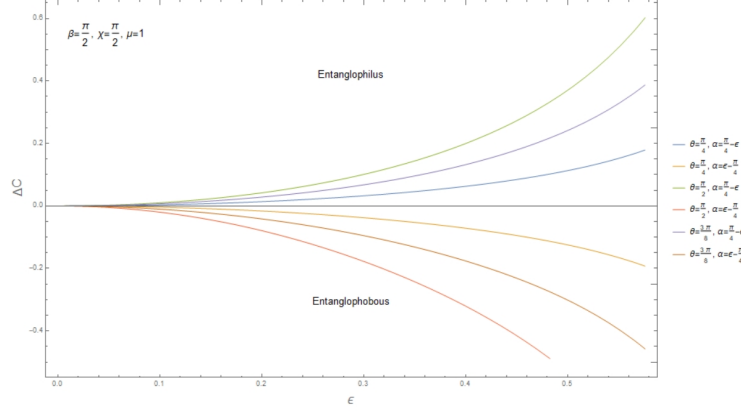


FIG. 6: Plot of  $\Delta C$  for states  $\Phi_\alpha^+$  (entanglophilus) and  $\Phi_\alpha^-$  (entanglophobus) as a function of  $\alpha$ .

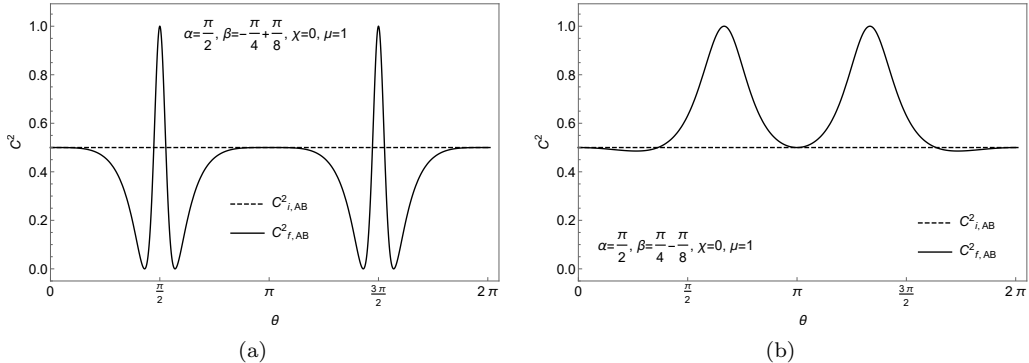


FIG. 7: Plot of  $\Delta C$  for states  $\Psi_\beta^+$  and  $\Psi_\beta^-$  as a function of  $\theta$ .

where  $\mathbf{N} = \sum_{\mathbf{rs}} \int_{\mathcal{D}} |\mathbf{M}(\mathbf{a}, \mathbf{b}; \mathbf{r}, \mathbf{s})|^2 \mathbf{d}\theta$  and  $Q = P, V, C$ .

Figs.8a-8c are relative to the initial state  $|RL\rangle$ . In this case, we have considered the relativistic limit for which, as shown in the plots 1d-1f, the entanglement is significantly different from zero in a very sharp region around  $\theta = \pi/2$ . So, we averaged the CCR terms in a neighborhood of  $\theta = \pi/2$  equal to  $\mathcal{D} \equiv \{\pi/2 - \pi/20, \pi/2 + \pi/20\}$ . It can be seen that if we narrow or widen the step from  $\theta = \pi/2$  the concurrence increases or decreases respectively, while predictability follows the reverse behavior. The triality relation Eq.(3) results verified also in this case.

## B. Interpretation

Here we give a qualitative glimpse about possible symmetries hidden in the conservation of maximum entanglement, and provide some analysis of the dynamics of the three quantum elements in the CCR in terms of probabilities and probability amplitudes.

We have seen that for scattering processes involving only spin-1/2 massive particles, maximum concurrence is completely conserved, while this is no more true for processes which include also spin-1 massless particles. Let us then assume the following, somewhat suggestive, point of view. The concurrence (see Eq. 9) can be interpreted as the modulus of the determinant of the  $2 \times 2$  matrix

$$M = \sqrt{2} \begin{pmatrix} a & b \\ c & d \end{pmatrix}, \quad (49)$$

where  $a, b, c, d$  are the coefficients of the general two-qubit state Eq.(4). For a maximally entangled state, the modulus of the determinant is 1 and it is simple to verify that the matrix  $M$  becomes an orthogonal matrix. The transformations  $T$  that send an orthogonal matrix in another orthogonal matrix are the isometries of the Orthogonal Group. For the

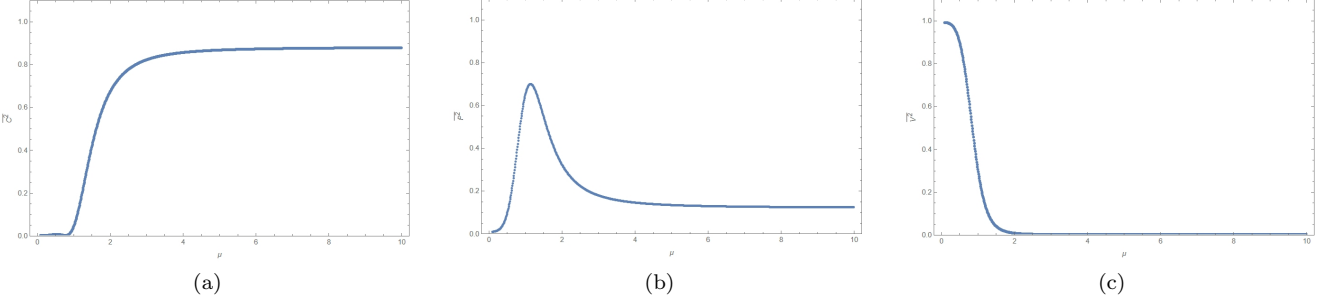


FIG. 8: Plot of the weighted average CCR terms as in definition Eq.(48) in the domain  $\mathcal{D}$ , as functions of the incoming momentum  $\mu$ .

first set of scattering processes, the output scattering amplitudes actually send the coefficient's matrix of an initial maximally entangled state into the final state by an orthogonal transformation matrix <sup>4</sup>. For processes involving photons, instead, this simple mechanism is partially, or totally, lost.

Moving to the analysis of the dynamics of CCR elements, we can write the latter in terms of probabilities and scattering amplitudes as

$$2P_{hs}(\rho_A) = P_A^2 = (P_{RR} - P_{LL})^2 + (P_{RL} - P_{LR})^2 - 2(P_{RR} - P_{LL})(P_{LR} - P_{RL}). \quad (50)$$

$$2C_{hs}(\rho_A) = V_A^2 = 4 \left( P_{RR}P_{LR} + P_{LL}P_{RL} + 2\sqrt{P_{RR}P_{LL}P_{RL}P_{LR}} \cos(\xi + \eta - \tau) \right) \quad (51)$$

$$2C_{hs}^{nl}(\rho_{A|B}) = C^2 = 4 \left( P_{RR}P_{LL} + P_{RL}P_{LR} - 2\sqrt{P_{RR}P_{LL}P_{RL}P_{LR}} \cos(\xi + \eta - \tau) \right) \quad (52)$$

with similar expressions for  $P_{hs}(\rho_B)$  and  $C_{hs}(\rho_B)$ . Here the probability  $P_{rs}$ ,  $r, s = R, L$  is obviously provided by the square modulus of the coefficient associated to the element  $|rs\rangle$ , while the phases  $\xi, \eta, \tau$  are associated to the terms  $|RL\rangle, |LR\rangle, |LL\rangle$ , respectively.

First of all, note that the predictability does not contain probability amplitudes but only probabilities, as is reasonable being this term associated to absence of quantum interference. On the contrary, the two local and nonlocal coherence measures, visibility and concurrence, contain amplitudes and phases just associated to quantum coherent interference, and the corresponding terms in the two quantities compensate each other in the sum. A very interesting situation happens when  $P_{RR} = P_{LL}$  and  $P_{RL} = P_{LR}$ : the predictability contribution Eq.(50) disappears, and only visibility and entanglement are present. From Eqs.(51) and (52) we see that, when the cosine is equal to 1, only the visibility contributions survive for any scattering angle. On the other hand, when the cosine is equal to  $-1$ , the state is a maximally entangled state for any scattering angle.

This mechanism is also present for other values of the cosine, but only for particular values of the scattering angle. In fact, consider the simplest case in which the expressions of visibility and concurrence are given by

$$2C_{hs}(\rho_A) = V_A^2 = 4 \left( P_{RR}P_{LR} + P_{LL}P_{RL} + 2\mathcal{M}(RR)\mathcal{M}(RL)\mathcal{M}(LR)\mathcal{M}(LL) \right) \quad (53)$$

$$2C_{hs}^{nl}(\rho_{A|B}) = C^2 = 4 \left( P_{RR}P_{LL} + P_{RL}P_{LR} - 2\mathcal{M}(RR)\mathcal{M}(RL)\mathcal{M}(LR)\mathcal{M}(LL) \right). \quad (54)$$

In Fig.9 we plot the case relative to the initial state  $|RR\rangle$  with  $\mu = \mu_{max} \equiv \frac{1}{2}\sqrt{-3 + \sqrt{17}}$ , while in Fig.10 the one relative to  $|RL\rangle$  in the limit for  $\mu = \infty$ . As we can see, when the probabilities are equal pairwise in the following way:  $P_{RR} = P_{LL}$  and  $P_{RL} = P_{LR}$ , then we obtain maximal entanglement and consistently  $P = V = 0$ . In the plots Fig.9 and Fig.10 we have reported the simplest cases corresponding to  $P_{RR} = P_{LL} = 1/2$ ,  $P_{RL} = P_{LR} = 0$  in  $\theta = \pi$  and  $P_{RL} = P_{LR} = 1/2$ ,  $P_{RR} = P_{LL} = 0$  in  $\theta = \pi/2, 3\pi/2$ , respectively.

<sup>4</sup> For example, in Bhabha scattering and for the Bell state  $\Phi^-$ , the final superposition results by an application on the initial matrix of coefficients of an orthogonal matrix  $T$  with determinant  $-1$  (and argument  $-s_1$  in the trigonometric terms of the matrix), while in Møller scattering and for the Bell state  $\Phi^+$ , the final superposition is obtained by applying an orthogonal matrix  $T$  with determinant  $1$  (in particular, a rotation of the angle  $s_3$ )

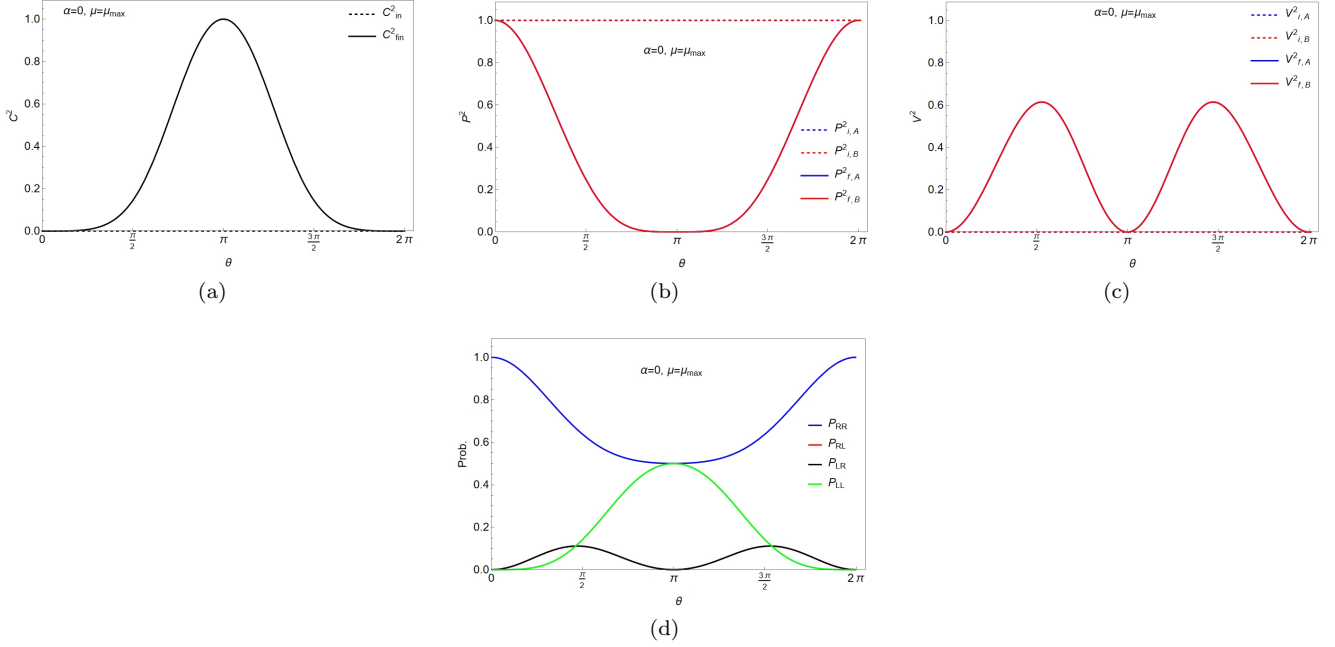


FIG. 9: Plot of CCR terms with respect to the probabilities behaviour, after scattering for the initial state  $|RR\rangle$  and  $\mu = \mu_{max}$

The analysis can be extended to the initial state  $|i\rangle_{II}$  and  $|i\rangle_{III}$  as in Eqs.(34) and (43). It turns out that the behaviour of probabilities are highly non-trivial, especially in the non-relativistic regime. Here, we report a particular initial configuration of parameter, that identify a sub-case of case II described by the state:

$$|i\rangle_{REF} = |R\rangle_A \otimes \frac{1}{\sqrt{2}}(|R\rangle_B + |L\rangle_B). \quad (55)$$

As it can be seen from Fig. 11 and in analogy with the previous case, we see that the points in which visibility is maximal correspond to those for which probabilities are  $P_{RR} = P_{LR} = 1/2$  and  $P_{RR} = P_{RL} = 1/2$ . Of course, when  $P_{RL} = P_{LR}$  in  $\theta = \pi/2, 3\pi/2$  (Fig. 11d), even if the value of probabilities is low, the corresponding entanglement at such  $\theta$  shows a peaks (Fig. 11a).

## VI. CONCLUSIONS AND OUTLOOK

In this work, we have analyzed the generation and transformation of entanglement in a QED scattering process at tree level, exploiting complete complementarity relations (CCR) which allow to take into account the intertwined evolutions of all quantum properties. Specifically, we focused on the Bhabha scattering process in the center-of-mass (COM) reference frame, where the particles are described by helicity states. We considered three distinct scenarios: the first, with the simplest factorized initial state; a second one, where the factorized initial state is expressed as a superposition of helicity states; and a third one, given by a more general case in which the particles are initially entangled in helicity.

The CCR, whose triality relation Eq. (3) is verified for both the initial and final states, provide a comprehensive characterization of the quantum aspects of a system composed of interacting elementary particles. Within this framework, we examined the interplay among the three elements of CCR, finding that their evolution after scattering is multifaceted and non-trivial, depending on the choice of the initial parameters.

More precisely, for the simplest factorized initial state, where only predictability exists before scattering, the other two CCR terms emerge in the non-relativistic limit, while only entanglement develops in the relativistic regime. This behavior persists even if the initial state exhibits only visibility. In this scenario, the two partitions of the system—electron and positron—display identical CCR behavior, as shown by coinciding plots.

The situation looks different in the case of initial factorized states with local coherence contributions, due to presence of interference terms in the two bipartitions just from the beginning as described in Eq. (34). The CCR terms for the

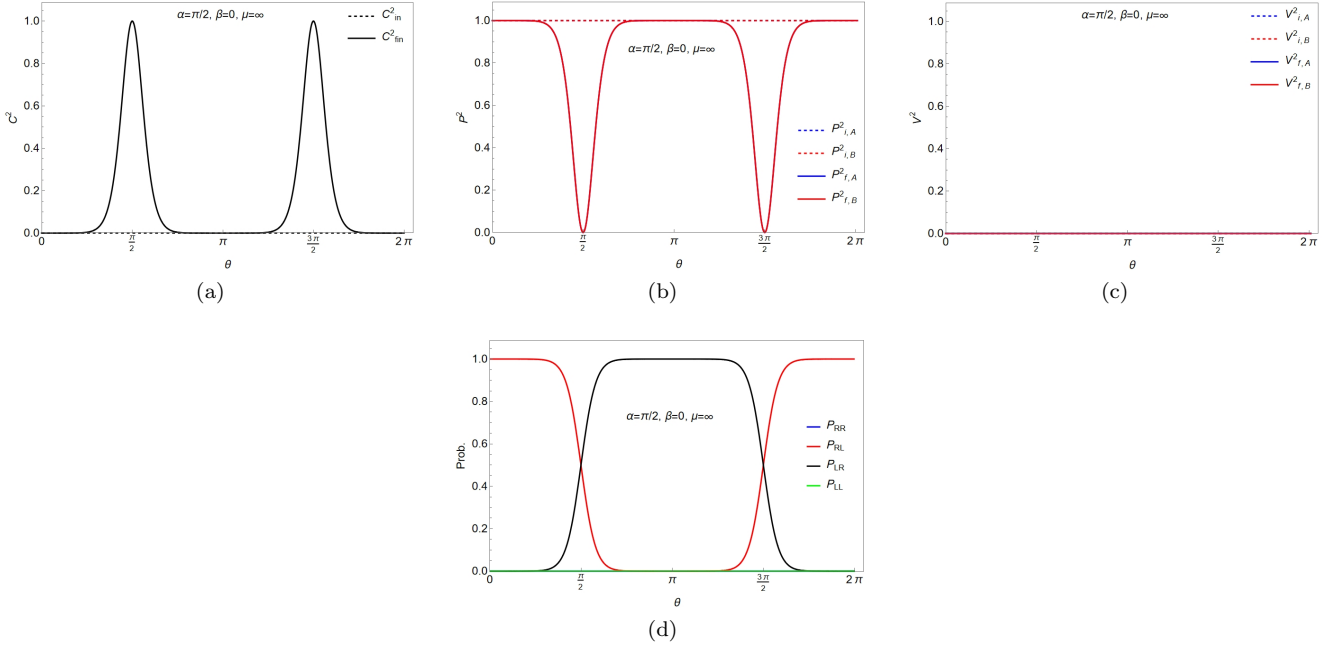


FIG. 10: Plot of CCR terms with respect to the probabilities behaviour, after scattering for the initial state  $|RL\rangle$  and  $\mu = \infty$

two bipartitions exhibit new non-trivial behaviors, resulting in asymmetry with respect to  $\theta = \pi$  in the non-relativistic regime, although such a symmetry is again restored in the relativistic regime.

The most significant results arise in the context of the third case, where the incoming particles are entangled. Depending on the initial parameters, after scattering we can distinguish four different regimes. The first, which we define *entanglophilus*, is characterized by increased final entanglement compared to the initial one for any scattering angle  $\theta$ . The second regime, which we term *entanglophobous*, shows instead reduced final entanglement with respect to the initial one for any scattering angle  $\theta$ . The third, the *mixed* regime, represents an intermediate situation between the last two, in which the increasing or decreasing of the final entanglement depend on the value of the scattering angle. These three patterns can be deduced starting from the two pairs of Bell states  $\Phi^\pm$  and  $\Psi^\pm$  Eq. (45) and gradually reducing the initial entanglement. The relative phase between the two states  $\Phi^\pm$  in the non-factorizable superposition determines which of the first two cases applies, while the same procedure for the pair  $\Psi^\pm$  leads to mixed regime.

This led eventually to the fourth scenario, involving maximally entangled states, which has been investigated not only in reference to the Bhabha scattering process as in the previous cases, but also for other QED scattering processes. We found that, for processes involving only massive spin-1/2 particles, if the initial state is prepared as a Bell state, or more in general as a state with maximal concurrence, the particles will remain maximally entangled for any value of the scattering angle (and of incoming momenta), and regardless of how many scattering processes they undergo. The situation looks different if also massless, spin 1 particles (photons) are present: depending on the process, only a partial conservation of maximal entanglement, or no conservation at all, is detected. A concise characterization of these aspects for all the processes is provided in Tables I-III, where the correspondences among initial and final states are reported for initial Bell states. All these behaviors are direct consequence of QED symmetries, a topic that we plan to explore further in a subsequent work [82].

To assess how the generation and transformation of entanglement could be exploited as a resource to create entangled particle pairs, we have investigate the Bhabha scattering process as a paradigmatic example. We demonstrate that, for a suitable range of scattering angles of an angular aperture of  $\pi/10$ , if one starts from the factorized state  $|RL\rangle$  and increases the incoming momentum, the square of the final concurrence stabilizes around an high value of about 0.8. This is just one example showing that, by adjusting the angular resolution of the experimental apparatus, one can select particles with a relevant level of entanglement.

Finally, some interpretation of the behavior of the CCR terms evolved after the scattering in terms of probability and probability amplitudes has been provided.

These results can have potential applications in experimental and technological contexts, and the study of CCR in

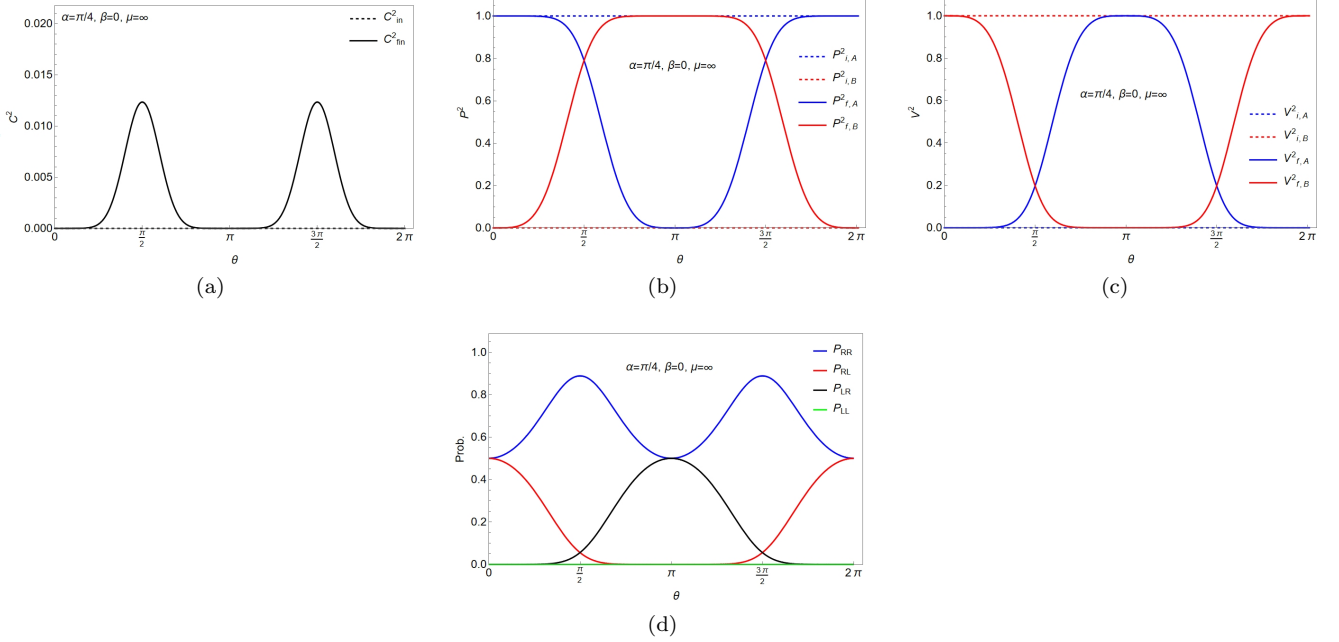


FIG. 11: Plot of CCR terms with respect to the probabilities behaviour, after scattering for the initial state Eq.(55) and  $\mu = \infty$ .

the realm of fundamental interactions can serve as a probe for testing the properties of QFT theories and beyond.

As future developments, it will be very interesting to extend investigations of the above aspects to other interactions beyond QED, and to study their formulation in different Lorentz reference systems.

### Appendix: QED scattering amplitudes

The scattering amplitudes are calculated in the COM reference frame of particles  $A$  and  $B$ . In the following,  $p_1 = (\omega, 0, 0, |\vec{p}|)$  and  $p_2 = (\omega, 0, 0, -|\vec{p}|)$  are the incoming 4-momenta that lie along the  $z$ -axis, while  $p_3 = (\omega, |\vec{p}| \sin \theta, 0, |\vec{p}| \cos \theta)$  and  $p_4 = (\omega, -|\vec{p}| \sin \theta, 0, -|\vec{p}| \cos \theta)$  are the outgoing four-momenta lying along a direction that form an angle  $\theta$  with respect to  $z$ -axis.  $a, b, r, s$  are the spin indices,  $\mu \equiv \frac{|\mathbf{p}|}{m_e}$ , where  $|\mathbf{p}|$  is the incoming momentum in the COM reference frame and  $m_e$  the electron mass.

### Bhabha scattering

$$\mathcal{M} = e^2 \left[ \bar{v}(b, p_2) \gamma^\mu u(a, p_1) \frac{1}{(p_1 + p_2)^2} \bar{u}(r, p_3) \gamma_\mu v(s, p_4) - \bar{v}(b, p_2) \gamma^\mu v(s, p_4) \frac{1}{(p_1 - p_3)^2} \bar{u}(r, p_3) \gamma_\mu u(a, p_1) \right] \quad (56)$$

$$\mathcal{M}(RR; RR) = \mathcal{M}(LL; LL) = \frac{(2 + 11\mu^2 + 8\mu^4 + 2\cos\theta + \mu^2\cos 2\theta) \csc^2(\frac{\theta}{2})}{4\mu^2(1 + \mu^2)} \quad (57)$$

$$\mathcal{M}(RR; {}_{LR}^{RL}) = -\mathcal{M}(LL; {}_{LR}^{RL}) = -\frac{(1 + \mu^2\cos\theta) \cot(\frac{\theta}{2})}{\mu^2\sqrt{1 + \mu^2}} \quad (58)$$

$$\mathcal{M}(RR; LL) = \mathcal{M}(LL; RR) = \frac{1 + \mu^2(1 + \cos\theta)}{\mu^2(1 + \mu^2)} \quad (59)$$

$$\mathcal{M}({}_{LR}^{RL}; RR) = -\mathcal{M}({}_{LR}^{RL}; LL) = \frac{(1 + \mu^2\cos\theta) \cot(\frac{\theta}{2})}{\mu^2\sqrt{1 + \mu^2}} \quad (60)$$

$$\mathcal{M}(RL; RL) = \mathcal{M}(LR; LR) = \frac{(1 + \mu^2(1 + \cos\theta)) \cot^2(\frac{\theta}{2})}{\mu^2} \quad (61)$$

$$\mathcal{M}(RL; LR) = \mathcal{M}(LR; RL) = 1 - \cos\theta - \frac{1}{\mu^2} \quad (62)$$

### Møller scattering

$$\mathcal{M} = e^2 \left[ \bar{u}(r, p_3)\gamma^\mu u(a, p_1) \frac{1}{(p_1 - p_3)^2} \bar{u}(s, p_4)\gamma_\mu u(b, p_2) - \bar{u}(r, p_3)\gamma^\mu u(b, p_2) \frac{1}{(p_2 - p_3)^2} \bar{u}(s, p_4)\gamma_\mu u(a, p_1) \right] \quad (63)$$

$$\mathcal{M}(RR; RR) = \mathcal{M}(LL; LL) = -\frac{(3 + 8\mu^2 + \cos 2\theta) \csc^2\theta}{\mu^2} \quad (64)$$

$$\mathcal{M}(RR; {}_{LR}^{RL}) = \mathcal{M}(LL; {}_{LR}^{RL}) = \mp \frac{2\sqrt{1 + \mu^2} \cot\theta}{\mu^2} \quad (65)$$

$$\mathcal{M}(RR; LL) = \mathcal{M}(LL; RR) = \frac{2}{\mu^2} \quad (66)$$

$$\mathcal{M}(RL; {}_{LL}^{RR}) = -\mathcal{M}(LR; {}_{LL}^{RR}) = \frac{2\sqrt{1 + \mu^2} \cot\theta}{\mu^2} \quad (67)$$

$$\mathcal{M}(RL; RL) = \mathcal{M}(LR; LR) = -(2 \cot^2 \frac{\theta}{2} + \frac{1}{\mu^2} \cos\theta \csc^2 \frac{\theta}{2}) \quad (68)$$

$$\mathcal{M}(RL; LR) = \mathcal{M}(LR; RL) = (2 \tan^2 \frac{\theta}{2} - \frac{1}{\mu^2} \cos\theta \sec^2 \frac{\theta}{2}) \quad (69)$$

$$e^- e^+ \rightarrow \mu^- \mu^+$$

$$\mathcal{M} = e^2 \left[ \bar{v}(b, p_2)\gamma^\mu u(a, p_1) \frac{1}{(p_1 + p_2)^2} \bar{u}(r, p_3)\gamma_\mu v(s, p_4) \right] \quad (70)$$

$$\mathcal{M}(RR; {}_{LL}^{RR}) = \mathcal{M}(LL; {}_{RR}^{LL}) = \mp \frac{\lambda \cos \theta}{\lambda^2 + \mu^2} \quad (71)$$

$$\mathcal{M}(RR; {}_{LR}^{RL}) = -\mathcal{M}(LL; {}_{LR}^{RL}) = \frac{\lambda \sin \theta}{\sqrt{\lambda^2 + \mu^2}} \quad (72)$$

$$\mathcal{M}({}_{LR}^{RL}; RR) = -\mathcal{M}({}_{LR}^{RL}; LL) = -\frac{\sin \theta}{\sqrt{\lambda^2 + \mu^2}} \quad (73)$$

$$\mathcal{M}(RL; RL) = \mathcal{M}(LR; LR) = -(1 + \cos \theta) \quad (74)$$

$$\mathcal{M}(RL; LR) = \mathcal{M}(LR; RL) = (1 - \cos \theta) \quad (75)$$

$$e^- \mu^- \rightarrow e^- \mu^-$$

$$\mathcal{M} = e^2 \left[ \bar{u}(s, p_4) \gamma^\mu u(b, p_2) \frac{1}{(p_1 - p_3)^2} \bar{u}(r, p_3) \gamma_\mu u(a, p_1) \right] \quad (76)$$

$$\mathcal{M}(RR; RR) = \mathcal{M}(LL; LL) = -\frac{\mu^2(3 - \cos \theta) + \sqrt{(1 + \mu^2)(\lambda^2 + \mu^2)}(1 + \cos \theta)}{\mu^2(-1 + \cos \theta)} \quad (77)$$

$$\mathcal{M}(RR; RL) = -\mathcal{M}(LL; LR) = \frac{\sqrt{\lambda^2 + \mu^2} \cot(\theta/2)}{\mu^2} \quad (78)$$

$$\mathcal{M}(RR; LR) = -\mathcal{M}(LL; RL) = -\frac{\lambda \sqrt{1 + \mu^2} \cot(\theta/2)}{\mu^2} \quad (79)$$

$$\mathcal{M}(RR; LL) = \mathcal{M}(LL; RR) = -\frac{\lambda}{\mu^2} \quad (80)$$

$$\mathcal{M}(RL; RR) = -\mathcal{M}(LR; LL) = -\frac{\sqrt{\lambda^2 + \mu^2} \cot(\theta/2)}{\mu^2} \quad (81)$$

$$\mathcal{M}(RL; LL) = -\mathcal{M}(LR; RR) = -\frac{\lambda \sqrt{1 + \mu^2} \cot(\theta/2)}{\mu^2} \quad (82)$$

$$\mathcal{M}(RL; RL) = \mathcal{M}(LR; LR) = \frac{\left( \mu^2 + \sqrt{(1 + \mu^2)(\lambda^2 + \mu^2)} \right) \cot^2(\theta/2)}{\mu^2} \quad (83)$$

$$\mathcal{M}(RL; LR) = \mathcal{M}(LR; RL) = \frac{\lambda}{\mu^2} \quad (84)$$

In the following we report the scattering amplitudes in the COM reference frame that involve photons as input and/or output state. In these cases the indices  $r$  and  $s$  are associated to the polarization  $\lambda = \pm 1$ . We can define the photons states expressed in circular basis as:  $|R\rangle \equiv \epsilon_{\lambda=+1}(\theta, \phi) = \frac{e^{i\phi}}{\sqrt{2}}(0, -\cos \theta \cos \phi + i \sin \phi, -\cos \theta \sin \phi - i \cos \phi, \sin \theta)$  and  $|L\rangle \equiv \epsilon_{\lambda=-1}(\theta, \phi) = \frac{e^{-i\phi}}{\sqrt{2}}(0, \cos \theta \cos \phi + i \sin \phi, \cos \theta \sin \phi - i \cos \phi, -\sin \theta)$ . In the scattering  $e^- e^+ \rightarrow \gamma\gamma$  we choose the outgoing photons momenta as  $p_3 = (\omega, \omega \sin \theta, 0, \omega \cos \theta)$  and  $p_4 = (\omega, -\omega \sin \theta, 0, -\omega \cos \theta)$ . In the case of Compton process the momentum of the outgoing photon is  $p_4 = (\omega, -\omega \sin \theta, 0, -\omega \cos \theta)$ .

$$e^- e^+ \rightarrow \gamma\gamma$$

$$\mathcal{M} = -e^2 \epsilon_\mu^*(s, p_4) \epsilon_\nu^*(r, p_3) \bar{v}(b, p_2) \left[ \frac{-\gamma^\mu p_3 \gamma^\nu + 2\gamma^\mu p_1}{-2p_1 \cdot p_3} + \frac{-\gamma^\nu p_4 \gamma^\mu + 2\gamma^\nu p_1}{-2p_1 \cdot p_4} \right] u(a, p_1) \quad (85)$$

$$\mathcal{M}(RR; RR) = -\mathcal{M}(LL; LL) = -\frac{4(\mu + \sqrt{1 + \mu^2})}{\mu^2(1 - \cos 2\theta) + 2} \quad (86)$$

$$\mathcal{M}(RR; LL) = -\mathcal{M}(LL; RR) = \frac{4(-\mu + \sqrt{1 + \mu^2})}{\mu^2(1 - \cos 2\theta) + 2} \quad (87)$$

$$\mathcal{M}(RR; RL) = \mathcal{M}(RR; LR) = \pm \frac{4\mu \sin^2 \theta}{\mu^2(1 - \cos 2\theta) + 2} \quad (88)$$

$$\mathcal{M}(RL; LL) = \mathcal{M}(LR; LL) = 0 \quad (89)$$

$$\mathcal{M}(RL; RL) = \mathcal{M}(LR; LR) = -\frac{2\mu\sqrt{1 + \mu^2}(1 + \cos \theta) \sin \theta}{1 + \mu^2 \sin^2 \theta} \quad (90)$$

$$\mathcal{M}(RL; LR) = \mathcal{M}(LR; RL) = \frac{2\mu\sqrt{1 + \mu^2}(1 - \cos \theta) \sin \theta}{1 + \mu^2 \sin^2 \theta} \quad (91)$$

### Compton scattering

$$\mathcal{M} = -e^2 \epsilon_\mu^*(s, p_4) \epsilon_\nu(r, p_2) \bar{u}(b, p_3) \left[ \frac{-\gamma^\mu p_2 \gamma^\nu + 2\gamma^\mu p_1}{2p_1 \cdot p_2} + \frac{-\gamma^\nu p_4 \gamma^\mu + 2\gamma^\nu p_1}{-2p_1 \cdot p_4} \right] u(a, p_1) \quad (92)$$

$$\mathcal{M}(RR; RR) = \mathcal{M}(LL; LL) = -\frac{4\mu \cos \theta/2 + 2(-\mu + \sqrt{1 + \mu^2}) \cos^3 \theta/2}{\mu \cos \theta + \sqrt{1 + \mu^2}} \quad (93)$$

$$\mathcal{M}(RR; RL) = \mathcal{M}(LL; LR) = -\frac{(-\mu + \sqrt{1 + \mu^2}) \cos \theta/2}{\mu \cos \theta + \sqrt{1 + \mu^2}} (1 - \cos \theta) \quad (94)$$

$$\mathcal{M}(RR; LR) = -\mathcal{M}(LL; RL) = \frac{1 + \cos \theta}{\mu \cos \theta + \sqrt{1 + \mu^2}} \sin \theta/2 \quad (95)$$

$$\mathcal{M}(RR; LL) = -\mathcal{M}(LL; RR) = \frac{2(-\mu + \sqrt{1 + \mu^2})^2}{\mu \cos \theta + \sqrt{1 + \mu^2}} \sin^3 \theta/2 \quad (96)$$

$$\mathcal{M}(RL; RR) = \mathcal{M}(LR; LL) = -\frac{(-\mu + \sqrt{1 + \mu^2}) \cos \theta/2}{\mu \cos \theta + \sqrt{1 + \mu^2}} (1 - \cos \theta) \quad (97)$$

$$\mathcal{M}(RL; LL) = -\mathcal{M}(LR; RR) = \frac{1 + \cos \theta}{\mu \cos \theta + \sqrt{1 + \mu^2}} \sin \theta/2 \quad (98)$$

$$\mathcal{M}(RL; RL) = \mathcal{M}(LR; LR) = -\frac{2(\mu + \sqrt{1 + \mu^2})}{\mu \cos \theta + \sqrt{1 + \mu^2}} \cos^3 \theta/2 \quad (99)$$

$$\mathcal{M}(RL; LR) = -\mathcal{M}(LR; RL) = \frac{2 \sin^3 \theta/2}{\mu \cos \theta + \sqrt{1 + \mu^2}} \quad (100)$$

- 
- [1] J. G. Ren et al., Ground-to-satellite quantum teleportation, *Nature* **549** (2017) 70.
- [2] J. Yin et al., Entanglement-based secure quantum cryptography over 1,120 kilometres, *Nature* **582** (2020) 501.
- [3] R. Jozsa and N. Linden, On the role of entanglement in quantum computational speed-up, *Proceedings of the Royal Society A: Mathematical, Physical and Engineering Sciences* **459** (2003) 2011.
- [4] R. Demkowicz-Dobrzanski and L. Maccone, Using entanglement against noise in quantum metrology, *Physical Review Letters* **113** (2014) 250801.

- [5] A. Osterloh, L. Amico, G. Falci, and R. Fazio, Scaling of entanglement close to a quantum phase transition, *Nature* **416** (2002) 608.
- [6] J. Eisert, M. Cramer, and M. B. Plenio, Area laws for the entanglement entropy - a review, *Rev. Mod. Phys.* **82** (2010) 277.
- [7] P. Calabrese and J. L. Cardy, Entanglement entropy and quantum field theory, *J. Stat. Mech.* **0406** (2004), P06002.
- [8] F. Benatti and R. Floreanini, Bell's locality and  $\epsilon'/\epsilon$ , *Physical Review D* **57** (1998), R1332.
- [9] R. A. Bertlmann and B. C. Hiesmayr, Bell inequalities for entangled kaons and their unitary time evolution, *Phys. Rev. A* **63** (2001), 062112.
- [10] R. A. Bertlmann, W. Grimus, and B. C. Hiesmayr, Bell inequality and CP violation in the neutral kaon system, *Phys. Lett. A* **289** (2001), 21.
- [11] R. A. Bertlmann and B. C. Hiesmayr, Kaonic Qubits, *Quantum Information Processing* **5** (2006) 421.
- [12] G. Amelino-Camelia et al., Physics with the KLOE-2 experiment at the upgraded DA $\phi$ NE, *Eur. Phys. J. C* **68** (2010) 619.
- [13] L. Lello, D. Boyanovsky, and R. Holman, Entanglement entropy in particle decay, *JHEP* **11** (2013) 116.
- [14] J. Bernabeu, A. Di Domenico and P. Villanueva-Perez, Direct test of time-reversal symmetry in the entangled neutral kaon system at a  $\phi$ -factory, *Nucl. Phys. B* **868** (2013), 102.
- [15] J. Bernabeu, A. Di Domenico and P. Villanueva-Perez, Probing CPT in transitions with entangled neutral kaons, *JHEP* **10** (2015), 139.
- [16] S. R. Beane, D. B. Kaplan, N. Klco, and M. J. Savage, Entanglement Suppression and Emergent Symmetries of Strong Interactions, *Phys. Rev. Lett.* **122** (2019) 102001.
- [17] Y. Afik and J. R. M. de Nova, *Phys. Rev. Lett.* **130** (2023) no.22, 221801
- [18] G. Aad et al. [ATLAS], *Nature* **633** (2024) no.8030, 542
- [19] M. Blasone, F. Dell'Anno, S. De Siena and F. Illuminati, On entanglement in neutrino mixing and oscillations, *J. Phys. Conf. Ser.* **237** (2010), 012007.
- [20] M. Blasone, F. Dell'Anno, S. De Siena, M. De Mauro, and F. Illuminati, Multipartite entangled states in particle mixing, *Physical Review D - Particles, Fields, Gravitation and Cosmology* **77** (2008), 096002.
- [21] M. Blasone, F. Dell'Anno, S. De Siena, and F. Illuminati, Entanglement in neutrino oscillations, *EPL* **85** (2009), 50002.
- [22] M. Blasone, F. Dell'Anno, S. De Siena, and F. Illuminati, Entanglement in a QFT model of neutrino oscillations, *Advances in High Energy Physics* **2014** (2014), 359168.
- [23] S. Banerjee, A. K. Alok, R. Srikanth, and B. C. Hiesmayr, A quantum-information theoretic analysis of three-flavor neutrino oscillations, *The European Physical Journal C* **75** (2015).
- [24] A. K. Alok, S. Banerjee and S. U. Sankar, Quantum correlations in terms of neutrino oscillation probabilities, *Nucl. Phys. B* **908** (2016), 352.
- [25] X.-K. Song, Y. Huang, J. Ling, M.-H. Yung, Quantifying quantum coherence in experimentally observed neutrino oscillations, *Phys. Rev. A* **98** (2018) 050302.
- [26] J. Naikoo, A.K. Alok, S. Banerjee, Leggett-Garg inequality in the context of three flavor neutrino oscillation, *Phys. Rev. D* **99** (2019) 095001.
- [27] K. Dixit, J. Naikoo, S. Banerjee, A.K. Alok, Study of coherence and mixedness in meson and neutrino systems, *Eur. Phys. J. C* **79**, (2019)96.
- [28] X.-K. Song, J. Ling, L. Ye, D. Wang, Entropic uncertainty relation in neutrino oscillations, *Eur. Phys. J. C* **80** (2020) 275.
- [29] M. Blasone, S. De Siena e C. Matrella, Wave packet approach to quantum correlations in neutrino oscillations, *Eur. Phys. J. C* **81** (2021) 660.
- [30] V. A. S. V. Bittencourt, M. Blasone, S. De Siena and C. Matrella, Complete complementarity relations for quantum correlations in neutrino oscillations, *Eur. Phys. J. C* **82** (2022), 66.
- [31] V. A. S. V. Bittencourt, M. Blasone, S. D. Siena and C. Matrella, Complete complementarity relations for three-flavor neutrino oscillations, *J. Phys. Conf. Ser.* **2533** (2023).
- [32] M. Duch, A. Strumia and A. Titov, New physics in spin entanglement, (2024) [arXiv:2403.14757 [hep-ph]].
- [33] K. Kowalska and E. M. Sessolo, Entanglement in flavored scalar scattering, *JHEP* **07** (2024), 156.
- [34] E. B. Manoukian and N. Yongram, Speed dependent polarization correlations in QED and entanglement, *Eur. Phys. J. D* **31** (2004) 137.
- [35] S. Ryu and T. Takayanagi, Holographic derivation of entanglement entropy from the anti-de sitter space/conformal field theory correspondence, *Phys. Rev. Lett.* **96** (2006) 181602.
- [36] K. Jensen and A. Karch, Holographic dual of an Einstein-Podolsky-Rosen pair has a wormhole, *Phys. Rev. Lett.* **111** (2013) 211602.
- [37] J. Maldacena and L. Susskind, Cool horizons for entangled black holes, *Fortschr. Phys.* **61** (2013) 201300020.
- [38] S. Bose et al., Spin entanglement witness for quantum gravity, *Phys. Rev. Lett.* **119** (2017) 240401.
- [39] C. Marletto and V. Vedral, Gravitationally induced entanglement between two massive particles is sufficient evidence of quantum effects in gravity, *Phys. Rev. Lett.* **119** (2017) 240402.
- [40] T. W. V. D. Kamp, R. J. Marshman, S. Bose, and A. Mazumdar, Quantum gravity witness via entanglement of masses: Casimir screening, *Phys. Rev. A* **102** (2020) 062807.
- [41] H. C. Nguyen and F. Bernards, Entanglement dynamics of two mesoscopic objects with gravitational interaction, *Eur. Phys. J. D* **74** (2020) 10077.
- [42] D. L. Danielson, G. Satischchandran, and R. M. Wald, Gravitationally mediated entanglement: Newtonian field versus gravitons, *Phys. Rev. D* **105** (2022) 086001.
- [43] A. Iorio, G. Lambiase, and G. Vitiello, Entangled quantum fields near the event horizon and entropy, *Ann. Phys.* **309**

- (2004) 151-165.
- [44] V. Balasubramanian, M. B. McDermott, and M. Van Raamsdonk, Momentum-space entanglement and renormalization in quantum field theory, *Phys. Rev. D* **86** (2012) 045014.
- [45] R. Peschanski and S. Seki, Entanglement Entropy of Scattering Particles, *Phys. Lett. B* **758** (2016) 89.
- [46] R. Peschanski and S. Seki, Evaluation of Entanglement Entropy in High Energy Elastic Scattering, *Phys. Rev. D* **100** (2019).
- [47] S. Seki, I. Y. Park, and S. J. Sin, Variation of Entanglement Entropy in Scattering Process, *Phys. Lett. B* **743** (2015), 147.
- [48] D. Carney, L. Chaurette and G. Semenoff, Scattering with partial information, (2016) [arXiv:1606.03103 [hep-th]].
- [49] R. Faleiro, H. A. S. Costa, R. Pavão, B. Hiller, A. H. Blin, and M. Sampaio, Perturbative approach to entanglement generation in QFT using the S matrix, *J. Phys. A* **53** (2020).
- [50] D. E. Kharzeev and E. M. Levin, Deep inelastic scattering as a probe of entanglement, *Phys. Rev. D* **95** (2017), 114008.
- [51] M. M. Altakach, P. Lamba, F. Maltoni, K. Mawatari and K. Sakurai, Quantum information and CP measurement in  $H \rightarrow \tau^+ \tau^-$  at future lepton colliders, *Phys. Rev. D* **107** (2023), 093002.
- [52] J. B. Araujo et al., Measuring QED cross sections via entanglement, *Phys. Rev. D* **100** (2019), 105018.
- [53] J. D. Fonseca, B. Hiller, J. B. Araujo, I. G. da Paz, and M. Sampaio, Entanglement and scattering in quantum electrodynamics: S matrix information from an entangled spectator particle, *Phys. Rev. D* **106** (2022), 056015.
- [54] N. Yongram, Spin correlations in elastic  $e^+ e^-$  scattering in QED, *Eur. Phys. J. D* **47** (2008), 71.
- [55] K. Beck and G. Jacobo, Comment on “Spin correlations in elastic  $e^+ e^-$  scattering in QED”, *Eur. Phys. J. D* **77** (2023), 85.
- [56] D. Gangopadhyay, D. Home and A. S. Roy, Probing the Leggett-Garg Inequality for Oscillating Neutral Kaons and Neutrinos, *Phys. Rev. A* **88** (2013) 022115.
- [57] D. Gangopadhyay and A. S. Roy, Three-flavoured neutrino oscillations and the Leggett–Garg inequality, *Eur. Phys. J. C* **77** (2017) 260.
- [58] S. Shivasankara, Entanglement Entropy of Compton Scattering with a Witness, *Can. J. Phys.* **101** (2023) 757.
- [59] G. M. Quinta e R. André, Multipartite Entanglement from Consecutive Scatterings, [arXiv:2311.11102 [quant-ph]].
- [60] R. A. Morales, Exploring Bell inequalities and quantum entanglement in vector boson scattering, *Eur. Phys. J. Plus* **138** (2023) 1157.
- [61] R. Aoude, E. Madge, F. Maltoni e L. Mantani, Probing new physics through entanglement in diboson production, *JHEP* **12** (2023) 017.
- M. Blasone, G. Lambiase and B. Micciola, Entanglement distribution in Bhabha scattering with an entangled spectator particle, *Phys. Rev. D* **109** (2024), 096022.
- [62] J. Fan and X. Li, Relativistic effect of entanglement in fermion-fermion scattering, *Phys. Rev. D* **97** (2018) 016011.
- [63] G. A. Miller, Entanglement maximization in low-energy neutron-proton scattering, *Phys. Rev. C* **108** (2023) L031002.
- [64] G. A. Miller, Entanglement of elastic and inelastic scattering, *Phys. Rev. C* **108** (2023) L041601.
- [65] A. Sinha e A. Zahed, Bell inequalities in 2-2 scattering, *Phys. Rev. D* **108** (2023) 025015.
- [66] A. Cervera-Lierta, J. I. Latorre, J. Rojo and L. Rottoli, Maximal Entanglement in High Energy Physics, *SciPost Phys.* **3** (2017), 036.
- [67] A. Cervera Lierta, Maximal Entanglement: Applications in Quantum Information and Particle Physics, (2019) [arXiv:1906.12099 [quant-ph]].
- [68] M. Blasone, G. Lambiase and B. Micciola, Entanglement distribution in Bhabha scattering with an entangled spectator particle, *Phys. Rev. D* **109** (2024), 096022.
- [69] S. Fedida e A. Serafini, Tree-level entanglement in quantum electrodynamics, *Phys. Rev. D* **107** (2023) 116007.
- [70] S. Fedida and A. Serafini, Entanglement entropy in scalar quantum electrodynamics, *Phys. Rev. D* **107** (2023), 116007.
- [71] S. Fedida, A. Mazumdar, S. Bose and A. Serafini, Entanglement entropy in scalar quantum electrodynamics, *Phys. Rev. D* **109** (2024), 065028.
- [72] N. Bohr, The Quantum Postulate and the recent Development of Atomic Theory, *Nature* **127** (1928) 580.
- [73] J-M. Lévy-Leblond, On the Nature of Quantons, *Science & Education* **12** (2003) 495.
- [74] W. K. Wootters e W. H. Zurek, Complementarity in the double-slit experiment: Quantum nonseparability and a quantitative statement of Bohr’s principle, *Phys. Rev. D* **19** (1979) 473.
- [75] B-G. Englert, Fringe Visibility and Which-Way Information: An Inequality, *Phys. Rev. Lett.* **77** (1996) 2154.
- [76] M. Jakob e J. A. Bergou, Generalized complementarity relations in composite quantum systems of arbitrary dimensions, *International Journal of Modern Physics B* **20** (2006) 1371.
- [77] M. Jakob e J. A. Bergou, Quantitative complementarity relations in bipartite systems: Entanglement as a physical reality, *Optics Communications* **283** (2010) 827.
- [78] M. L. W. Basso e J. Maziero, Complete complementarity relations for multipartite pure states, *J. Phys. A* **53** (2020) 465301.
- [79] M. L. W. Basso e J. Maziero, Complete complementarity relations and their Lorentz invariance, *Proc. Roy. Soc. Lond. A* **477** (2021) no. 2253, 20210058.
- [80] M. L. W. Basso e J. Maziero, Entanglement monotones connect distinguishability and predictability, *Phys. Lett. A* **425** (2022) 127875.
- [81] M. E. Peskin and D. V. Schroeder, “An Introduction to quantum field theory”, Addison-Wesley, 1995.
- [82] M. Blasone, S. De Siena, G. Lambiase, C. Matrella and B. Micciola, work in progress.